

## EFFECTS OF DIFFERENT PARAMETERS ON DED HR-1 ON LOW CYCLE FATIGUE, TENSILE STRENGTH, AND MICROSTRUCTURE

J. Lares<sup>1,2</sup>, D. Godinez<sup>1,2</sup>, E. Arrieta<sup>1</sup>, F. Medina<sup>1</sup>, R. Wicker<sup>1</sup>, P. Gradl<sup>3</sup>, C. Katsarelis<sup>3</sup>

W.M. Keck Center for 3D Innovation, The University of Texas at El Paso, TX 79968, USA.

[jelaresmona@miners.utep.edu](mailto:jelaresmona@miners.utep.edu)

<sup>1</sup>W.M. Keck Center for 3D Innovation, El Paso, TX, 79968

<sup>2</sup>Metallurgical and Materials Engineering at the University of Texas at El Paso, El Paso, TX, 79968

<sup>3</sup>NASA Marshall Space Flight Center, Huntsville, AL 35812, USA

**Keywords:** *NASA HR-1, Direct Energy Deposition (DED), deposition parameters, microstructure*

### Abstract

NASA HR1 alloy is an iron-nickel based material designed by NASA and derived from A286 and JBK-75 alloys. At extreme conditions, NASA HR1 possess high strength, high fatigue resistance, and high resistance to corrosion and hydrogen embrittlement. The main applications include structural components and liquid rocket engine nozzles with internal cooling channels. NASA has produced HR1 using vacuum induction melting (VIM), a considerably expensive fabrication method. Aimed to explore other more affordable and accessible manufacturing methods, HR1 specimens were fabricated under different parameters using Laser-Powder Directed Energy Deposition (LP-DED) and were heat treated through stress relief, homogenization, solution treatment and aging. The feasibility of this AM process was investigated by evaluating mechanical and microstructural analysis on specimens. This work finalizes with discussion and remarks on tensile and low-cycle fatigue properties and its relationship with microstructural features.

### Introduction

HR1 is mainly composed of Fe-Ni-Cr has been used in liquid engine rockets components such as cooling nozzles [1,2]. This alloy has been produced traditionally using vacuum induction melting [1]. Alternative manufacturing technologies are being explored to substitute this process, reducing costs. However, all manufacturing technologies provide mechanical properties that must be considered for its application to make sure this component will experience any deformation or fracture when being in service. Laser Powder Direct Energy Deposition (LP-DED) is one of the additive manufacturing (AM) technologies being analyzed since it can reduce the cost mentioned before and it allows to create complex and large geometries. Before using DED as the default manufacturing technology for cooling nozzles, it is important to study the mechanical properties that HR1 acquires through this process and how this can be improved. The main purpose of this project is to evaluate the impact of using different laser power and angle deposition parameters on microstructure, tensile strength, and low cycle fatigue performance of NASA HR1 LP-DED. To

analyze these effects, NASA has created different plates deposited at two different power settings, including 1070 W and 2620 W but also the angle at which powder is being melted varied from 0, 20 and 30 degrees as represented in **figure 1**. 12 plates were printed in total by creating 2 plates of each power/angle combination, for instance, 1070 W 0°, 1070 W 20°, 2620 0°, and so on. In addition, all these plates have been heat treated according to NASA HR 1 cycle which involved stress relief for 1.5 hours, homogenization for 6 hours in vacuum, solution treatment for 1 hour in vacuum and finally aging treatment.

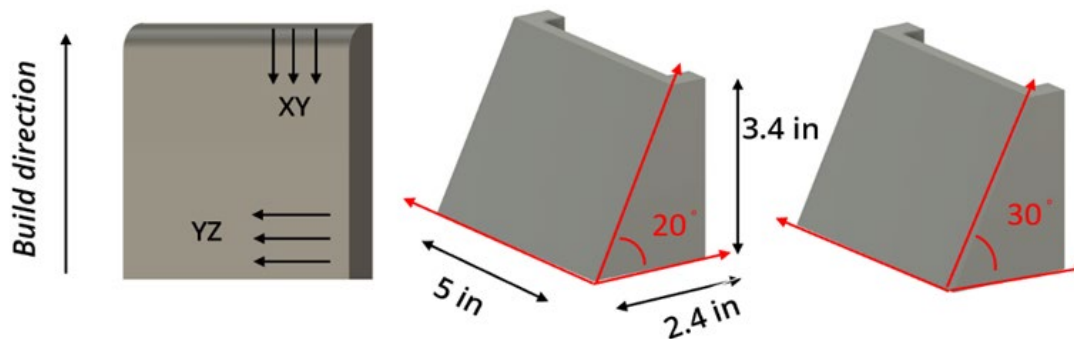


*Figure 1 CAD model representation of plates printed at different angles.*

## Materials and methods

### Metallography

Metallographic preparation was required to see the microstructure of all different plates and compare their differences if found. All plates were sectioned in such a way planes XY (parallel to build lines) and XZ (build direction) could be observed. All samples were hot mounted, then, grinded from 240 to 600 grit to then be polished using diamond suspension of 9  $\mu\text{m}$ , 3  $\mu\text{m}$ , and 0.1  $\mu\text{m}$ . Once a mirror surface was observed, these were taken to an optical microscope to appreciate the porosity differs between the ones deposited at 1070 W and 2620 W. Three images of each sample taken under the microscope were used to calculate their density using ImageJ software. Furthermore, etching was completed using Kallings #2 etchant for about three minutes to see the microstructure on both planes.

### Mechanical Testing

All plates have been sectioned as mentioned before to get different bars that were subjected to tensile and low cycle fatigue testing as shown in **figure 2**. These plates were sectioned and marked at W. M. Keck Center and then sent to Astro Laboratories in Los Angeles, CA to be tested there. This laboratory oversaw machining the 3D printed plates until having four tensile bars and three fatigue bars of each power/angle combination with the appropriate dimensions and shape. It was reported that both mechanical testing was performed per ASTM E8-22 and ASTM e606-21 standards until fracture for tensile and low cycle fatigue respectively.

## Results and discussion

### Defects and microstructure analysis

Porosity was measured along XY plane in all specimens to compare the density percentage. It was observed that between those samples printed at 1070 W had similar densities ranging from 99.92% to 99.98%. However, those printed at 2620 W showed densities from 99.79% to 99.85% being slightly lower. As seen in **figure 3**, the number of pores (indicated with red arrows) and also, they looked bigger in diameter, approximately 5% bigger. This may be an effect of gas getting entrapped easier in deeper melt pools when increasing wattage [2], which in this case, is more than double power.

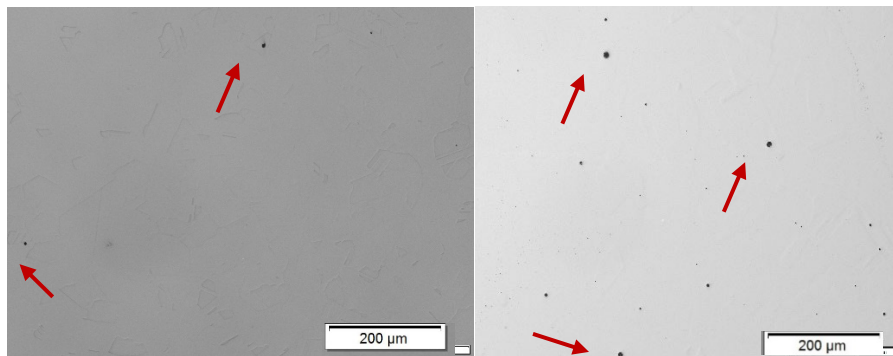


**Figure 3** Left picture obtained from a 1070 W and right image gotten from 2620 W sample.

As mentioned before, all plates (12 total, 2 of each power/angle combination) have gone through the same heat treatment. Therefore, it was expected that microstructure was similar in all plates. However, since the metal powder was deposited at different laser power, the solidification processes were different and thus the as-built microstructures [1]. As shown in literature, before heat treatment, a dendritic microstructure is appreciated being titanium rich in dark areas. It is also shown that increasing power also increases the depth and width of melt pools since the cooling rate is lower allowing these melt pools to grow [3]. Heat treatment plays an essential role in this paper since it has been evaluated if even when all plates have been printed at different angles and power settings, they have gotten a similar microstructure after heat treatment and, therefore, mechanical properties are similar as well. As shown in **figure 4**, all samples have an austenitic microstructure.

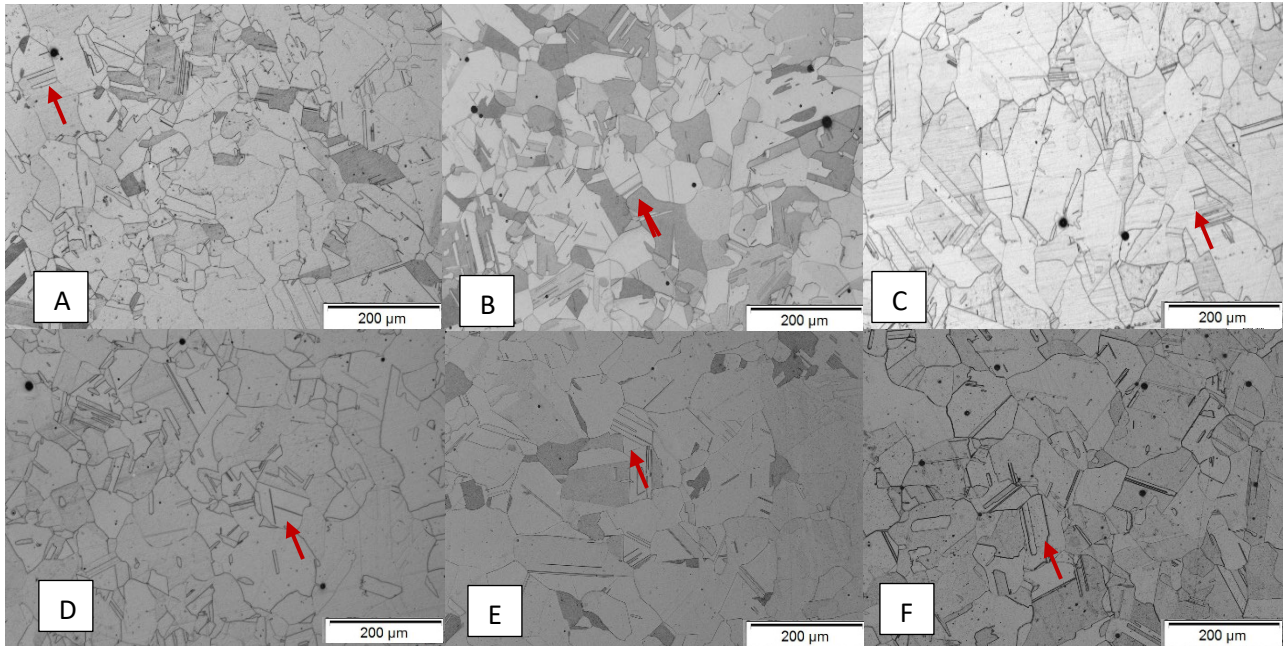


**Figure 4** Microstructure of HR1 manufactured with LP-DED at different settings including A) 1070 W 0 Degrees, B) 1070 W 20 Degree, C) 1070 W 30 Degrees, D) 2620 W 0 Degree, E) 2620 W 20 Degree, F) 2620 W 30 Degree

It is appreciated that dendrites have been completely removed in all samples by heat treatment and similar average grain size of 2.13 ASTM. Titanium might take longer to diffuse from grain boundaries to the bulk of the grains, making this diffusion dependent on the grain size [3]. In all cases, grain size ranged from 1.85 to 2.16 ASTM. In addition, annealed twinning (as indicated with red arrows) were found in all microstructures most likely due to the homogenization step. These twins contribute to increasing strength by pinning dislocations. Therefore, it is important to compare if they are present in all microstructures, which was the case. Since all microstructures are similar in terms of grain shape and size but also the presence of annealed twinning, it was expected to see similar mechanical behavior.

## Mechanical Testing

### *Tensile behavior*

Different average tensile properties, including 0.2% yield strength (YS), ultimate tensile strength (UTS), modulus of elasticity (E), and elongation percentage are illustrated in **table 1**. As expected, there is little difference between those plates with more than double laser power. Using both 0 degree plates as reference to be compared, 1070 W bars showed an average YS of 100 Ksi with a standard deviation of 1.08 Ksi and UTS of 159.4 Ksi with a 1.43 Ksi deviation while 2620 W bars showed a YS 97 Ksi and UTS 158.9 Ksi with standard deviation 0.39 Ksi and 2.09 Ksi

respectively. In terms of ductility, the higher wattage provided a slightly higher ductility by elongating approximately 2.5% more than the original length even though ductility may be affected by lower density. However, as reported by Colton, et al., AM materials ductility is affected only if the material porosity is 5% or higher [1].

Specimen	Average Ultimate Tensile Strength (Ksi)	Standard Deviation	Average 0.2% Yield Strength (Ksi)	Standard Deviation	Average Modulus of Elasticity (Msi)	Standard Deviation	Average Elongation (%)	Standard Deviation (Ksi)
0 Degree 1070 W	159.4	1.08	100.73	1.43	8.41	1.50	37.8	2.53
20 Degree 1070 W	153.9	3.38	96.9	1.71	9.83	3.25	43.8	0.85
30 Degree 1070 W	158.6	1.02	98.38	2.42	8.25	0.83	44.3	1.55
0 Degree 2620 W	158.9	0.39	96.98	2.09	9.42	1.79	35.3	2.63
20 Degree 2620 W	156.3	3.4	94.8	2.60	11.61	2.66	32.3	7.63
30 Degree 2620 W	155.3	1.16	90.3	1.31	12.4	1.77	41.0	0.96

**Table 1.** Results from tensile strength testing

Furthermore, samples with the same laser power (1070 W) starting with 20-degree sample showed a 3% lower UTS and YS than sample with 0 degrees. However, it elongated 6% more than the corresponding sample. On the other hand, the 30-degree sample has a similar ultimate tensile strength, and yield strength to the 0-degree specimen, a difference close to 1% for both properties. Moreover, 30 degrees plates elongated 6% more than the 0-degree sample. Having similar tensile data can be attributed to the heat treatment homogenizing the microstructures for all power/angle combination.

### Low Cycle Fatigue

As mentioned before, HR1 is used in applications such as cooling nozzles. Since they are part of the propulsion system of liquid engine rockets, they are exposed to high cyclic stresses. Therefore, the number of cycles required to failure was measured by reversal cycles to a 1% strain range and 0.5 Hz of frequency. As seen in **table 2**, the results for fatigue bars from 2620 W plates are graphically represented. Varying the angle from 0 to 20 degrees increased the number of cycles required to failure by 1100 reversal cycles. However, when the 30-degree sample withstood 5,500 cycles. In other words, there is a statistical difference between the number of cycles that 0- and 20-degree samples, but 30 degrees sample did not show to follow this trend. This difference may be a result of an error or variation during mechanical testing.



Specimen	No of Reversal Cycles (Average of three samples)
0 Degrees 10170 W	4800
30 Degrees 1070 W	5100
0 Degrees 2620 W	4700
20 Degrees 2620 W	5800
30 Degrees 2620 W	5500

**Table 2.** Comparison of average number of reversal cycles needed to fail.

### Fractography

SEM was used to analyze the fracture surface along all different power/angle configuration. **Figure 6** shows how one of the tensile bars' surfaces that was selected randomly from 0-degree plate has fractured. A high number of gas entrapped pores were appreciated at the center of the surface (indicated with red arrows). In addition, dimples are also seen throughout the whole surface as proof of a ductile fracture mechanism. These dimples which indicate micro-void coalescence mechanism [4], were seen by increasing the magnification to 1000X. There was not a significant difference between all tensile specimens in terms of fracture surface. Fatigue bars were not included in this literature since they have not been analyzed under the scanning electron microscope yet.

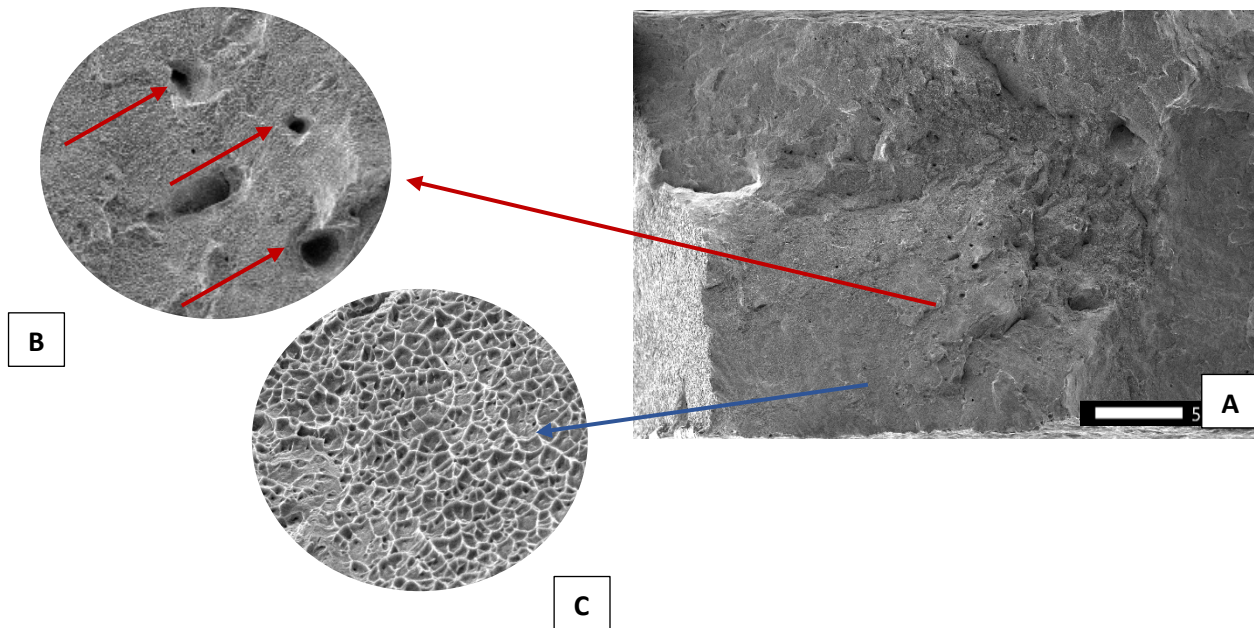


**Figure 6.** A) Fractography images obtained using scanning electron microscope. B) Gas-entrapped pores found at surface. C) Dimples and cone-cup shape surface

## Conclusion

This literature examined the defect content, microstructure, and mechanical properties of HR1 printed with Laser Powder Direct Energy Deposition at two different power settings, 1070 W and 2620 W and at three different deposition angles including 0, 20, and 30 degrees. Based on the results, the following conclusions have been derived:

- Increasing laser power increases the width and depth of melt pools, increasing the defective content on the material. However, the difference is not significant enough to affect ductility.
- NASA HR1 heat treatment was effective to homogenize the microstructure in all samples by providing a similar austenitic microstructure with similar grain size and shape.
- Similar microstructure provided, as expected, similar mechanical properties in terms of tensile strength and low cycle fatigue having no statistical difference.
- Fractography proved that titanium segregation was not present in any of the samples due heat treatment homogenization since all specimens had dimples showing a ductile fracture mechanism present at fractured surfaces.

## REFERENCES

- [1] C. Katsarelis, P. Chen, P. Gradl, C. Protz, Z. Jones, Additive Manufacturing of NASA HR-1 Material for Liquid Rocket Engine Component Applications
- [2] A. Soltani-Tehrani, P. Chenc, C. Katsarelis, P. Gradl, S. Shaoa, N. Shamsaei, Laser powder directed energy deposition (LP-DED) NASA HR-1 alloy: Laser power and heat treatment effects on microstructure and mechanical properties, Additive Manufacturing Letters 3 (2022)
- [3] P. Chen, C. Katsarelis, W. Medders, P. Gradl Segregation Evolution and Diffusion of Titanium in Directed Energy Deposited NASA HR-1, NASA/TM-20210013649 (2021)
- [4] A. Soltani-Tehran, P. Chen, C. Katsarelis, P. Gradl, S. Shao, N. Shamsaei Mechanical properties of laser powder directed energy deposited NASA HR-1 superalloy: Effects of powder reuse and part orientation, Thin-Walled Structures 185 (2023)
- [5] A. Gamon, E. Arrieta, P. Gradl, C. Katsarelis, L. Murr, R. Wicker, F. Medina, Microstructure and hardness comparison of as built inconel 625 alloy following various additive manufacturing processes (2021)
- [6] A. Mostafaei, C. Zhao, Y. He, S. Reza Ghiaasiaan, Bo Shi, S. Shao, N. Shamsaei, Z. Wu, N. Kouraytem, T. Sun, J. Pauza, J. V. Gordon, B. Webler, N. D. Parab, M. Asherloo, Q. Guo, L. Chen, A. D. Rollett, Defects, and anomalies in powder bed fusion metal additive manufacturing, (2022)